E-Journal of Advanced Maintenance Vol.11 No.2 (2019) pp.65-78
Japan Society of Maintenology

Evaluation of Capabilities on Ultrasonic Testing Examiners Using Probability of Defect Detection and Cumulative Failure Probability

Masayoshi KOJIMA[1,*], Hideharu TAKAHASHI[1] and Hiroshige KIKURA[1]

[1] *Tokyo Institute of Technology, 2-12-1-N1-7 Ookayama, Meguro-ku, Tokyo 152-8550, Japan*

ABSTRACT

Ultrasonic testing (UT) is one of the non-destructive testing for pressure-retaining weld lines in class 1 piping of nuclear power plants. Since capabilities of UT examiners may affect failure risks of class 1 piping, UT is performed by certified examiners. In this paper, capabilities of uncertified and certified examiners were evaluated using probability of detection (POD) models and cumulative failure probabilities. The POD models is one of the input data of probabilistic fracture mechanics (PFM) analysis. Experimental data of blind testing for detecting stress corrosion cracking conducted by the uncertified and certified examiners were used for regression analysis of POD model. Two types of equation were selected for the POD model. Cumulative failure probabilities considering several inspection intervals were calculated in the PFM analysis. Then, the authors evaluated the failure risks of piping performed by the uncertified and certified examiners using the POD models and the cumulative failure probabilities. As a result, one equation of POD model with low residual sum of squares made it easier to evaluate the capabilities of UT examiners than the other POD model. Additionally, the equation with low residual sum of squares had less uncertainty on the failure risks of piping. Furthermore, it was shown that UT results performed by certified examiners might have equivalent failure risks of piping as UT results performed by uncertified examiners if an inspection interval gets longer.

KEYWORDS

Failure Risk of Piping, Probability of Detection, Probabilistic Fracture Mechanics, Cumulative Failure Probability, Capabilities of Examiners, Ultrasonic Testing, Stress Corrosion Cracking, 95% Confidence Intervals

ARTICLE INFORMATION

Article history:
Received 7th May 2019
Accepted 30th August 2019

1. Introduction

Piping in nuclear power plants (NPPs) is generally subjected to non-destructive testing for their maintenance management. Ultrasonic testing (UT) is conducted at pressure-retaining weld lines of class 1 piping in NPPs [1]. Since capabilities of UT examiners may affect failure risks of class 1 piping, the UT is performed by certified examiners. Probabilistic fracture mechanics (PFM) analysis is one of the useful methods to evaluate the failure risks of piping. The PFM analysis has been studied for considering an inspection interval of the UT in a piping of primary loop recirculation (PLR) system of a boiling water reactor (BWR) in recent years. Machida [2] showed effects of probability factors, which were related to the JSME S NA1-2008 (Rules on Fitness-for-Service for Nuclear Power Plants) [3], on a reliability of the PLR piping. Cumulative failure probabilities were calculated using several virtual models of probability of detection (POD) in the PFM analysis. The conclusion showed reliable detection to large defect size is important to avoid piping failure. Shohji et al. [4] showed effects of cumulative failure probabilities in a case where the maximum POD was less than 1.0 (100%). Cumulative failure probabilities were also calculated using several virtual POD models. The conclusion showed the cumulative failure probabilities of the PLR piping were low if the defect height was around 8 mm or less even though the maximum POD was 0.9 (90%). However, the authors considered that the necessity of an evaluation regarding the effect on the failure risks of piping due to the difference in the capabilities of the UT examiners using POD model of experimental data has been remained. The POD is generally modeled by the regression analysis using results of defect detection measured by the UT examiners [5]. Several previous studies referred the POD models using UT results of blind testing for weld lines of austenitic stainless steel piping [2, 5, 6]. The results of blind

*Corresponding author, E-mail: kojima.m.al@m.titech.ac.jp

ISSN-1883-9894/10

testing are related to UT examiners' capabilities; therefore, it is necessary to grasp effects on the failure risks of piping using experimental data of blind testing considering the UT examiners' capabilities.

The objective of this paper is to evaluate effects on the failure risks of piping using experimental data considering the difference of the UT examiners' capabilities. First, the authors organized experiments of UT examinations to obtain experimental data of uncertified examiners. The uncertified examiners conducted the experiments for detecting stress corrosion cracking (SCC) at weld lines of piping. An experimental data of previous study for detecting SCCs conducted by certified examiners [7] were investigated and utilized as well. Then, the authors calculated POD models using both experimental data. Two types of equation were selected for the POD models. In addition, cumulative failure probabilities were calculated in the PFM analysis considering several inspection intervals. Finally, the authors evaluated effects on the failure risks of piping using the cumulative failure probabilities and the POD models considering the difference of the UT examiners' capabilities.

2. Methods

2.1. Experiments of Ultrasonic testing examinations

The UT examinations of the uncertified examiners were performed by 9 university students with no experience of manual UT for detecting SCC. The examiners conducted blind testing in which the locations and size of defects were not informed them. All the uncertified examiners participated in an UT training program organized by Nondestructive Evaluation Center of the Japan Power Engineering Inspection Corporation (JPEIC). The training was scheduled before the blind testing. Table 1 shows the outline of the training program. The training for detecting fatigue cracking in the carbon steel piping and SCCs in austenitic stainless steel piping was organized for 24 hours in total.

Table 1 Outline of lecture and practical training program organized by Nondestructive Evaluation Center of the JPEIC for uncertified examiners before conducting the experiments

	Items	Contents		Hours
Lecture	Basics of ultrasonic testing (UT)	1. Basics of UT 2. UT instrument		3.0
Lecture	Outline of UT	1. Procedure of UT 2. Calibration of UT instrument	3. Angle beam technique 4. Analysis of results	3.0
Practice	Calibration of UT instrument in angle beam technique	1. Probe index and angle of refraction by STB 2. Calibration of measurement range	3. Calibration sensitivity and distance-amplitude correction	1.5
Practice	UT to welded part of carbon steel plate	1. Angle beam technique 2. Data collection	3. Analysis	4.5
Lecture Practice	Outline of UT to weld of austenitic stainless steel (SUS) piping	1. Characteristic of UT on weld of SUS 2. Stress Corrosion cracking (SCC)	3. Important points on UT of SUS 4. Difference between carbon steel and SUS	2.0
Practice	Calibration of UT instrument in angle beam technique	1. Conversion of refraction angle 2. Re-calibration of measurement range	3. Calibration sensitivity and distance-amplitude correction	1.0
Practice	UT to weld of SUS piping	1. Angle beam technique 2. Data collection	3. Analysis 4. Extraction of defect echo	6.0
Lecture Practice	Feedback on the results of practice	1. Feedback on the results of practice 2. Explanation of key points in SCC detection		1.5
Lecture Practice	Secondary creeping wave	1. Principle, application and role 2. Calibration of UT instrument	3. Important points on handling of probe	1.5
			Total	24.0

Table 2(a) shows the examination conditions of the blind testing conducted by the uncertified examiners [8, 9]. The room temperature of an air conditioner during the blind testing was set to 24°C. SCCs at the welding heat affected zone (HAZ) in 350A piping of the SUS304 grade stainless steel were detected in the blind testing. 10 test specimens were prepared for the blind testing. 11 locations

of SCC in 7 test specimens were existed. There was no SCC in 3 test specimens. The 11 locations of SCC were identified as UE001 to UE011. Each examiner randomly selected 4 test specimens in the blind testing.

Table 2 Examination conditions of UT by (a) uncertified examiners and (b) certified examiners for calculations of POD

Items	**(a) Uncertified Examiners**	**(b) Certified Examiners** [7]
Examiner	9 university students	6 teams
Inspection guideline	JEAC 4207-2008 [8]	JEAC 4207-2004 [10]
Scanning	Manual scanning	Manual scanning: 5 teams Automatic scanning: 1 team
Probe technique	Single probe technique Angle beam technique	Single probe technique Angle beam technique and normal beam technique
Instrument	Digital UT instrument (UI-25IIb (Ryosho Electronics))	Digital or analog UT instrument
Probe	Shear wave normal probe Frequency:2MHz Mode: Shear wave Angle: 45deg Element size: 10x10mm (Type: 2Z10x10A45 (Japan Probe) or 2C10x10A45 (KGK))	Shear wave normal probe Frequency:2MHz Mode: Shear wave Angle: 45deg Element size: 10x10mm (Type: 2Z10x10A45)
Couplant	Glycerin paste (SONI COAT BS-400 (Taiyo Nippon Sanso Gas & Welding))	Glycerin paste
Calibration block	STB-A1 (JIS Z 2345-1 [9])	STB-A1 (JIS Z 2345-1 [9])
Reference block	SUS304, 25t (Side drilled hole: ϕ 2.4x1)	P350A-25t-SUS304 (Side drilled hole: ϕ 2.4x1)
Test specimen	Stainless steel piping welds specimen (350A, t25) Material: SUS304 grade stainless steel Size: ϕ 355.6mm x L400mm x 14.5deg(≒W90mm) Welding procedure: TF + A Defect: SCC (Position: Heat-affected zone) Number of specimens: 10 Number of SCCs: 11 (ID: UE001 ~ UE011) Weld groove shape: 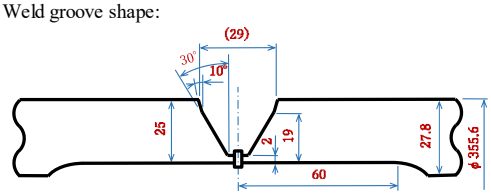	Stainless steel piping welds specimen (350A, t25) Material: SUS304 grade stainless steel Size: ϕ 355.6mm x L1200mm Welding procedure: - Defect: SCC (Position: Heat-affected zone) Number of specimens: - Number of SCCs: 12 (ID: PSS21 ~ PSS29, PSS2A ~ PSS2C) Weld groove shape: 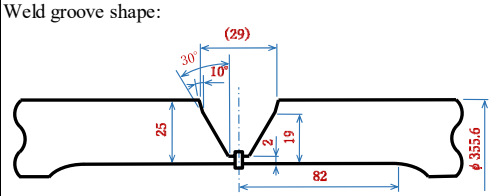
Testing period	About 1 hour / test specimen / person	1 week / team

The largest defect height measured by 3 types of probes was defined as the defect height of the 11 locations of SCC; where 3 types of probes were the shear wave end echo method using a fixed angle probe, the longitudinal wave end echo method using a fixed angle probe, and the longitudinal wave end echo method using a phased array probe. Although 2 locations of SCC (UE006 and UE009) were not detected by either of the 3 type of probes, they were detected by the liquid penetrant testing. The authors defined the defect height of the 2 SCCs as 1.5 mm; since the wavelength of 1 cycle in the UT examination is calculated to be 1.55 mm from values of the shear wave velocity in the austenitic stainless steel (3,100 m/s) and the frequency of the shear wave probe (2MHz), the authors predicted the wavelength of 1 cycle was the detection limit in the examination conditions. The authors expected the defined defect height of the 2 SCCs was 0.05 mm smaller than the predicted detection limit.

Procedure for detecting SCCs followed the JEAC 4207-2008; therefore, the uncertified examiners adjusted a sensitivity of the ultrasonic instrument, searched a unit exit point and a beam angle of a probe, drew a distance amplitude correction (DAC) curve, recorded all point of levels

greater than 20% of a DAC curve, and evaluated all the suspected flaw indications considering the point of reflection for detecting a SCC.

Experimental data for detecting SCCs conducted by certified examiners, which were organized by the Japan Nuclear Energy Safety Organization (JNES) [7], were investigated and utilized for comparison with the results of the uncertified examiners. Table 2(b) shows the examination conditions of UT by 6 teams of the certified examiners [7, 9, 10]. All the certified examiners had the certification of the non-destructive testing of UT Level 2 or 3, and have had experiences of in-service inspection (ISI) in the NPPs [7]. Test specimens with 12 locations of SCCs at the HAZ were examined [7].

2.2. Models of probability of detection

The POD model was defined as an equation of a defect height a. 2 types of equation of POD models with 1 regression coefficient and 2 regression coefficients were used for input data of the PFM analysis. The equation with 1 regression coefficient was defined as Model-1 described by Eq. (1) [11]. The equation with 2 regression coefficients was defined as Model-2 described by Eq. (2) [5].

Model-1

$$\begin{aligned} &POD(a) = 1 - \exp\left[-(a-\beta)\right] \\ &\beta_0, \quad \beta_{-95\%CL}, \quad \beta_{+95\%CL} \\ &se_\beta, \quad Se \end{aligned} \tag{1}$$

Model-2

$$\begin{aligned} &POD(a) = \left[1 + \exp\left(-\beta 1 - \beta 2 \times a\right)\right]^{-1} \\ &\beta 1_0, \quad \beta 1_{-95\%CL}, \quad \beta 1_{+95\%CL} \\ &\beta 2_0, \quad \beta 2_{-95\%CL}, \quad \beta 2_{+95\%CL} \\ &se_{\beta 1}, \quad se_{\beta 2}, \quad Se \end{aligned} \tag{2}$$

where, a (mm) is a defect height of SCC. β, $\beta 1$, and $\beta 2$ are regression coefficient. β_0, $\beta 1_0$, and $\beta 2_0$ are regression coefficient that minimized residual sum of squares. $\beta_{-95\%CL}$, $\beta_{+95\%CL}$, $\beta 1_{-95\%CL}$, $\beta 1_{+95\%CL}$, $\beta 2_{-95\%CL}$, and $\beta 2_{+95\%CL}$ are regression coefficient in 95% confidence intervals. se_β, $se_{\beta 1}$, and $se_{\beta 2}$ are standard errors. Se is a residual sum of squares in β_0, $\beta 1_0$, and $\beta 2_0$.

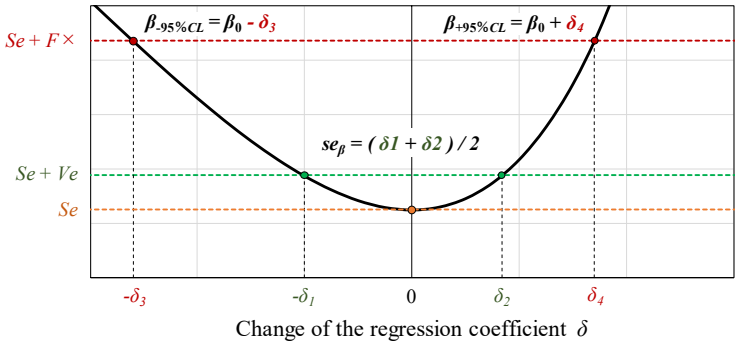

Fig. 1. Concept of profile likelihood approach for calculating the standard error and 95% confidence intervals

Fig. 1 shows a concept of profile likelihood approach for calculating the standard error and 95% confidence intervals [12]. Se (the residual sum of squares) is the sum of the squared difference between all the experimental data and equation of POD model calculated by the regression analysis.

Se (the standard error) is calculated from $-\delta_1$ and δ_2 which are the negative / positive change of the regression coefficients at $Se + Ve$ ($Ve = Se / n$: mean square for error, n: degrees of freedom of residual in the equation). The standard error is the arithmetic mean of δ_1 and δ_2; therefore, the calculated standard error called the approximate standard error [12]. The 95% confidence intervals are calculated from $-\delta_1$ and δ_2 at $Se + F \times Ve$ ($F = F_{0.05}(1, n)$: Snedecor's F-distribution at 0.05 significance level with 1 numerator degrees of freedom and n denominator degrees of freedom). The 95% lower confidence intervals are the sum of the regression coefficient and $-\delta_3$, and the 95% upper confidence intervals are the sum of the regression coefficient and δ_4.

The algorithms for the calculation of the standard error and 95% confidence intervals using the profile likelihood approach followed the Appendix I and II of the "Application of Nonlinear Regression Model to Sigmoid Dose-Response Relationship in Pharmacological Studies" [13]; here, the equation of sigmoid function using 4 regression coefficients ($\beta_1, \beta_2, \beta_3,$ and β_4) in those Appendices was replaced by Eq. (1) and Eq. (2) in the calculation process. The generalized reduced gradient (GRG) nonlinear method built in Microsoft Office Excel solver add-in was used in those calculations.

2.3. Calculation of cumulative failure probability

Cumulative failure probabilities of a SCC growth in a piping were calculated using a PFM analysis software. The software was written by the authors in visual basic for applications (VBA) built in Microsoft Office Excel. The software was referred the JSME S NA1-2008 [3] and previous studies [2, 4, 6, 14-20], and was verified comparing the analysis results of previous studies [6, 16].

Table 3 Analysis conditions of PFM for calculation of cumulative failure probabilities

Items	Analysis Conditions	References
Analyzed pipe (referring to Fig. 2)	400A Sch100 (16B Sch100) Pipe outside diameter: D_O = 406.4 (mm) Wall thickness: t = 26.2 (mm) Material: 316Lgrade stainless steel	
Failure mode	Stress Corrosion Cracking (SCC)	
Stress intensity factor K (MPa$\sqrt{}$m)	JSME S NA1-2008 (Att.E-5 5.3(1))	[3]
Crack height reaching weld metal dc (mm) (referring to Fig. 2)	$dc = L + \alpha$	[2, 16, 17]
Distance from weld metal to a SCC L (mm) (referring to Fig. 2)	Median: μ_L = 1.15 Standard deviation: σ_L = 1.39 (Log-normal distribution)	[2, 16, 17]
Adding length α (mm)	Median: μ_α = 2.99 Standard deviation: σ_α = 1.31 (Normal distribution)	[2, 16, 17]
SCC growth rate in heat-affected zone (HAZ) da/dt (m/s) (referring to Fig. 2)	$da/dt = C \cdot K^m$	[2, 3, 16]
	Exponent: m = 2.161 (Constant)	[2, 3, 16]
	Coefficient: C	
	C = 0 (K<0)	[3]
	Median: $\mu_{CHAZ} = 9.018 \times 10^{-14}$ (K≧0) Standard deviation: σ_{CHAZ} = 0.303 (Log-normal distribution)	[2, 16]
SCC growth rate in weld metal da/dt (m/s) (referring to Fig. 2)	$da/dt = C \cdot K^m$	[2, 3, 16]
	Exponent: m = 2.161 (Constant)	[2, 3, 16]
	Coefficient: C	
	C = 0 (K<0)	[3]
	Median: $\mu_{CWM} = 1.017 \times 10^{-14}$ (K≧0) Standard deviation: σ_{CWM} = 1.120 (Log-normal distribution)	[2, 16]
Normal operating loads (MPa)	Internal pressure p = 9.0 Membrane stress σ_m = 34.9 Bending stress σ_b = 10.0 Thermal expansion stress σ_e = 40.0	[16]

Table 3 shows the analysis conditions of PFM for calculating cumulative failure probabilities [2, 3, 16, 17]. Eq. (1) and Eq. (2) of both uncertified and certified examiners were used for the analysis input conditions as well. The piping material was defined SUS316L grade stainless steel [6, 16].

Fig. 2 shows a concept of a SCC growth in a HAZ and a weld metal of the SUS316L grade stainless steel piping [2, 16, 17]. The thickness (26.2 mm) of the 400A piping in the PLR system of BWR was close to the thickness (25.0 mm) of the 350A piping in the UT blind testing. Since the fatigue crack growth is small, that was not considered in the PFM analysis [4].

Stress due to welding residual stress, internal pressure, membrane stress, bending stress and thermal expansion stress were considered in the main factors contributing to the SCC growth [2, 3, 16]. Welding residual stress distribution in 400A austenitic stainless steel piping of the PLR system in BWR was utilized from the results of finite element method (see Fig. 3) [18, 19].

The authors defined an initial defect size as 0.01 mm in depth and 0.02 mm in length in the PFM analysis. Extrapolated values at the aspect ratios of 0.1 and 0.2 were used for the correction factor G [3] of the surface defect if the aspect ratio was less than 0.1 [19]. The failure of piping (leak or break of the piping) was defined in a case where the defect height was larger than the 75% of wall thickness [2, 4, 6].

The operating period was defined 40 years [6, 16]. The inspection intervals of 4, 5, 8, and 10 years were selected for the analysis input conditions. Pre-service inspection was not considered for the analysis. Time step size was 0.1 years. Sample size of Monte Carlo simulation was 10^6. The Failure probability per 1 sample was defined the calculation result of multiplying all of the probability of non-detection (PND: 1- POD) at the time of inspection in a case where the piping was failure [14, 17, 20]. The cumulative failure probabilities were calculated in the PFM analysis.

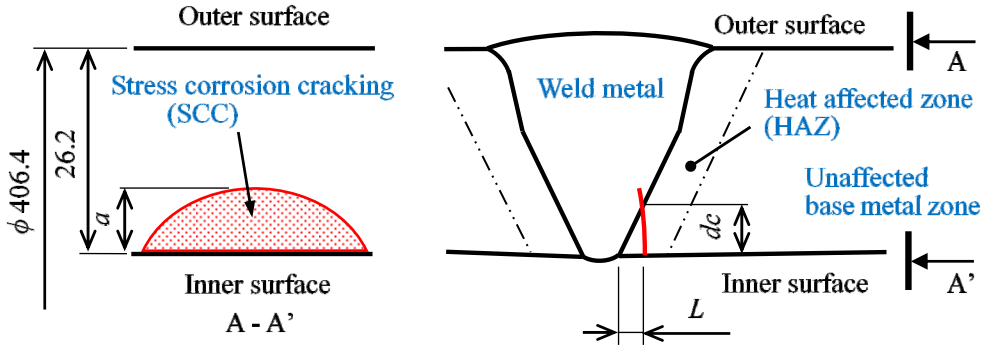

Fig. 2. Concept of SCC growth in HAZ and weld metal of SUS316L grade stainless steel piping [2, 16, 17]

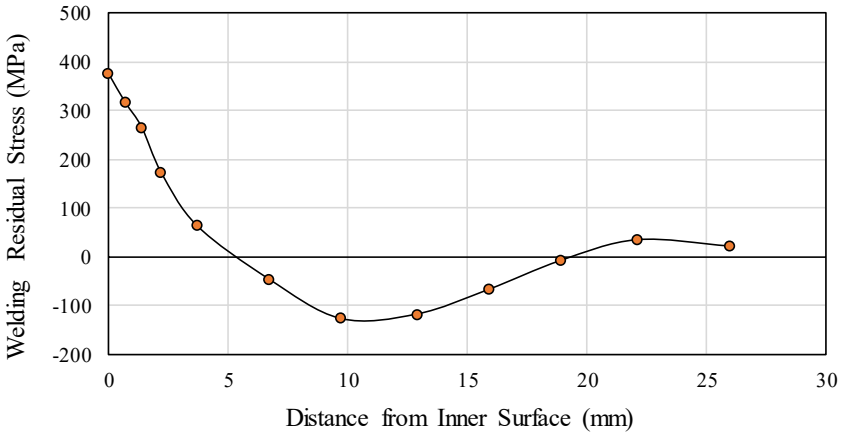

Fig. 3. Welding residual stress distribution of 400A austenitic stainless steel piping in PLR system [18, 19]

3. Results

3.1 Ultrasonic testing examinations

Table 4 shows the examination results of UT conducted by (a) the uncertified examiners and (b) the certified examiners [7].

Table 4 Examination results of UT for SCCs in SUS304 grade stainless steel 350A piping conducted by (a) uncertified examiners and (b) certified examiners

(a) Uncertified examiners

ID	Defect height a (mm)	Probability of defect detection $POD(a)$
UE001	7.5	1.00
UE002	2.0	1.00
UE003	8.0	1.00
UE004	2.0	0.60
UE005	1.8	0.50
UE006	1.5	0.00
UE007	4.2	1.00
UE008	5.8	0.75
UE009	1.5	0.00
UE010	2.0	1.00
UE011	4.3	0.80

(b) Certified examiners [7]

ID	Defect height a (mm)	Probability of defect detection $POD(a)$
PSS21	2.0	1.00
PSS22	2.1	1.00
PSS23	3.9	1.00
PSS24	2.4	1.00
PSS25	2.0	1.00
PSS26	2.4	1.00
PSS27	0.6	0.17
PSS28	3.6	1.00
PSS29	3.3	1.00
PSS2A	1.4	1.00
PSS2B	2.7	1.00
PSS2C	0.7	0.00

3.2 Probability of detection

Eqs. (3)-(6) show the equation of the Model-1 and Model-2 calculated from the examination results of UT conducted by the uncertified and certified examiners in Table 4.

Model-1 of the uncertified examiners

$$\begin{aligned} &POD(a) = 1 - \exp\left[-\left(a - \beta\right)\right] \\ &\beta_0 = 1.17, \quad \beta_{-95\%CL} = 0.649, \quad \beta_{+95\%CL} = 1.51 \\ &se_\beta = 0.184, \quad Se = 0.625 \end{aligned} \tag{3}$$

Model-2 of the uncertified examiners

$$\begin{aligned} &POD(a) = \left[1 + \exp\left(-\beta 1 - \beta 2 \times a\right)\right]^{-1} \\ &\beta 1_0 = -19.0, \quad \beta 1_{-95\%CL} = \mathrm{N/A}, \quad \beta 1_{+95\%CL} = -8.72 \\ &\beta 2_0 = 10.5, \quad \beta 2_{-95\%CL} = 4.93, \quad \beta 2_{+95\%CL} = \mathrm{N/A} \\ &se_{\beta 1} = 8.51, \quad se_{\beta 2} = 4.67, \quad Se = 0.213 \end{aligned} \tag{4}$$

Model-1 of the certified examiners

$$POD(a) = 1 - \exp\left[-(a - \beta)\right]$$
$$\beta_0 = 0.331, \quad \beta_{-95\%CL} = -0.0938, \quad \beta_{+95\%CL} = 0.630 \tag{5}$$
$$se_\beta = 0.159, \quad Se = 0.363$$

Model-2 of the certified examiners

$$POD(a) = \left[1 + \exp\left(-\beta 1 - \beta 2 \times a\right)\right]^{-1}$$
$$\beta 1_0 = -8.82, \quad \beta 1_{-95\%CL} = \text{N/A}, \quad \beta 1_{+95\%CL} = -5.73$$
$$\beta 2_0 = 8.93, \quad \beta 2_{-95\%CL} = 5.75, \quad \beta 2_{+95\%CL} = \text{N/A} \tag{6}$$
$$se_{\beta 1} = 3.71, \quad se_{\beta 2} = 4.41, \quad Se = 0.0252$$

where, N/A stands for the not available; since the change of the regression coefficient δ did not reach $Se + F \times Ve$, the 95% confidence intervals were not calculated (see Figs. 4 and 5).

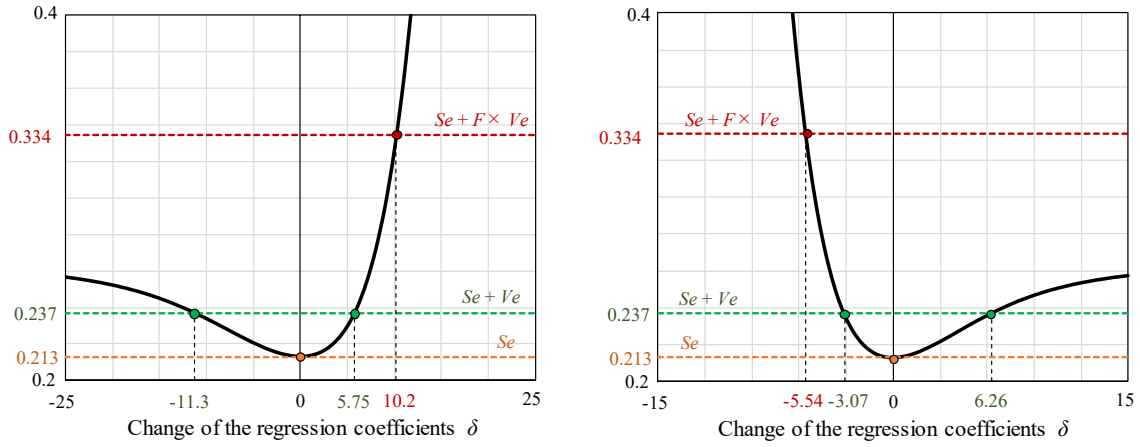

(a) $\beta 1$ **(b) $\beta 2$**

Fig. 4. Profile likelihood approach for calculating 95% confidence intervals of (a) $\beta 1$ and (b) $\beta 2$ in Eq. (4)

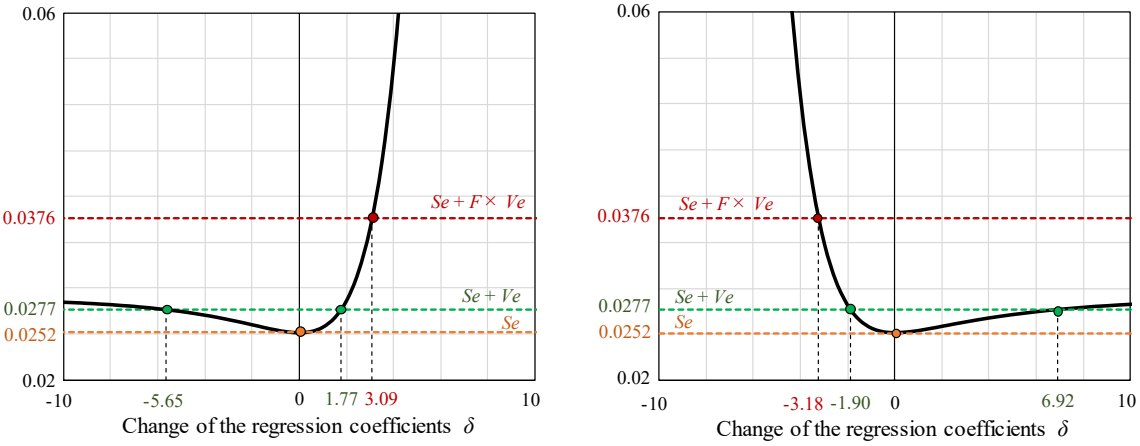

(a) $\beta 1$ **(b) $\beta 2$**

Fig. 5. Profile likelihood approach for calculating 95% confidence intervals of (a) $\beta 1$ and (b) $\beta 2$ in Eq. (6)

Although $\beta 1_{-95\%CL}$ and $\beta 2_{+95\%CL}$ were not calculated in Eqs. (4) and (6), equations of the 95% confidence intervals are described as Eqs. (7) and (8). This is because the residual sum of squares in Eqs. (7) and (8) are as equal as the $Se + F \times Ve$ in Eqs. (4) and (6).

Model-2 of the uncertified examiners at 95% confidence intervals in Eq. (4)

$$\begin{aligned} POD(a) &= \left[1+\exp\left(-\beta 1_{+95\%CL} - \beta 2_{-95\%CL} \times a\right)\right]^{-1} \\ \beta 1_{+95\%CL} &= -8.72, \quad \beta 2_{-95\%CL} = 4.93 \\ Se_{95\%CL} &= Se + F \times Ve = 0.213 + 5.12 \times 0.0237 = 0.334 \\ n &= n_{UE} - n_1 = 11 - 2 = 9 \end{aligned} \tag{7}$$

Model-2 of the certified examiners at 95% confidence intervals in Eq. (6)

$$\begin{aligned} POD(a) &= \left[1+\exp\left(-\beta 1_{+95\%CL} - \beta 2_{-95\%CL} \times a\right)\right]^{-1} \\ \beta 1_{+95\%CL} &= -5.73, \quad \beta 2_{-95\%CL} = 5.75 \\ Se_{95\%CL} &= Se + F \times Ve = 0.0252 + 4.96 \times 0.00252 = 0.0376 \\ n &= n_{CE} - n_1 = 12 - 2 = 10 \end{aligned} \tag{8}$$

where, $Se_{95\%CL}$ is the residual sum of squares in Eqs. (7) and (8). Se is the residual sum of squares in Eqs. (4) and (6) in $\beta 1_0$ and $\beta 2_0$. Ve is the mean square for error in Eqs. (4) and (6) in $\beta 1_0$ and $\beta 2_0$. F is the Snedecor's F-distribution in Eqs. (4) and (6) in $\beta 1_0$ and $\beta 2_0$. n_{UE} is the number of SCC locations in UT examination by uncertified examiners. n_{CE} is the number of SCC locations in UT examination by certified examiners. n_1 is the number of the regression coefficient in Eqs. (4) and (6).

Fig. 6 (a) shows the PODs of the Model-1 described by Eqs. (3) and (5). Fig. 6 (b) shows the PODs of the Model-2 described by Eqs. (4) and (8). The horizontal axis is the defect height a (mm). The vertical axis is the POD. UE stands for the uncertified examiners, and CE stands for the certified examiners. The red circles are the examination results conducted by the uncertified examiners. The yellow triangles are the examination results conducted by the certified examiners.

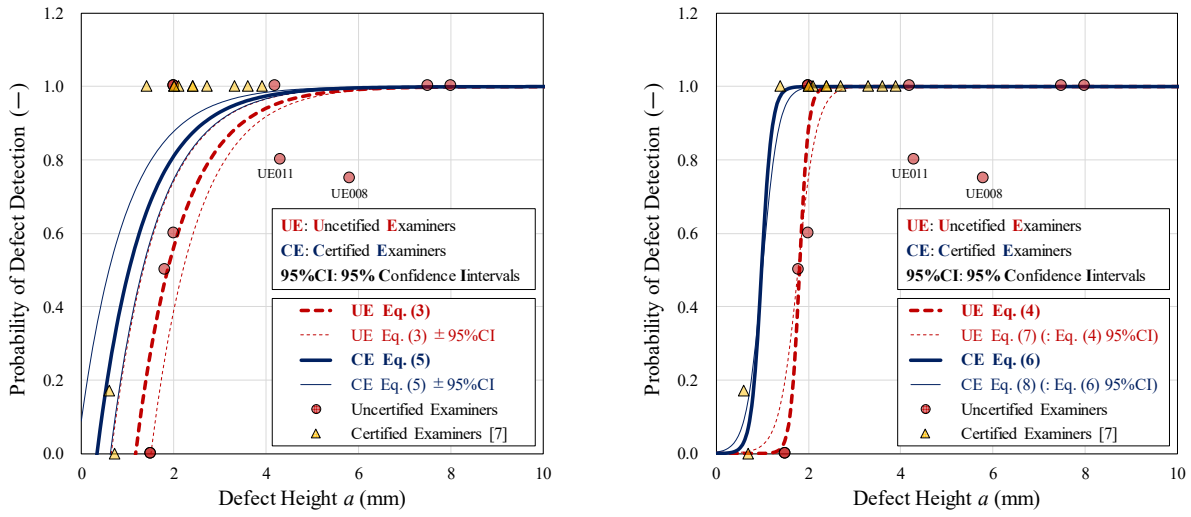

(a) Model-1 **(b) Model-2**

Fig. 6. POD results of (a) Model-1 and (b) Model-2

3.3 Cumulative failure probability

Fig. 7 shows the analysis results of cumulative failure probability after 40 years' operation. Fig. 7 (a) shows the results of the Model-1, and Fig. 7 (a) shows the results of the Model-2. The horizontal axis is the inspection interval (years). The vertical axis is the cumulative failure probability (crack $^{-1}$). The green circles are the uncertified examiners' results of β_0. The white circles are the uncertified examiners' results of the 95% confidence intervals. The yellow triangles are the certified examiners' results of β_0. The white triangles are the certified examiners' results of the 95% confidence intervals.

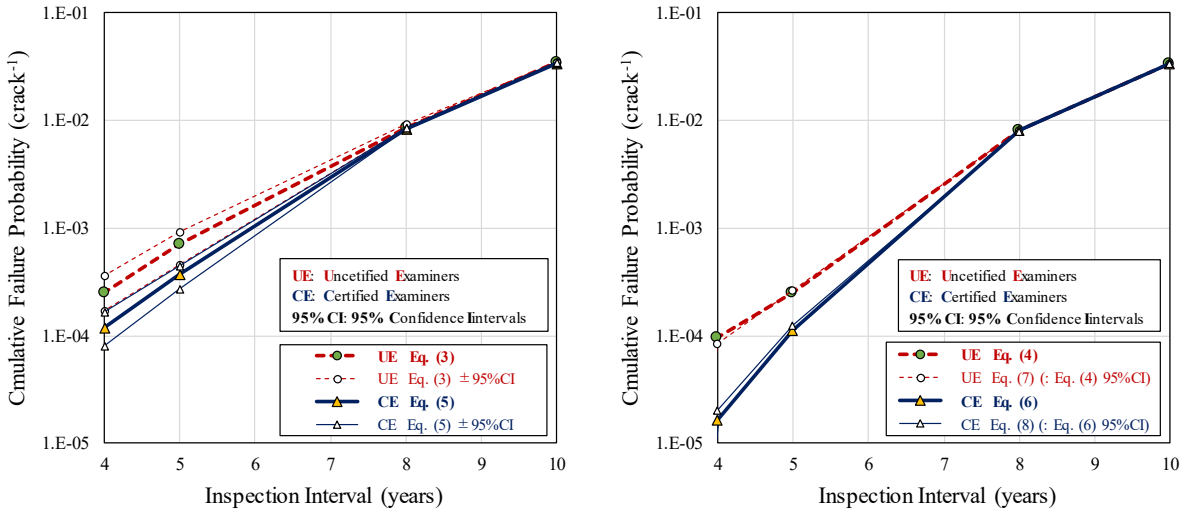

(a) Model-1 **(b) Model-2**

Fig. 7. PFM analysis results of (a) Model-1 and (b) Model-2 on cumulative failure probabilities

4. Discussion

4.1 Evaluation of capabilities using experimental data of UT examiners

Eqs. (3)-(6) showed the superiority of the Model-2; the residual sum of squares of the Model-2 was clearly lower than that of Model-1. In addition, Fig. 6 showed that the Model-2 had narrow range of the 95% confidence intervals than that of the Model-1.

The examination results in Table 4(b) showed that the certified examiners detected all defects of height equal to or greater than 2 mm. In contrast, even though the defect height of UE008 and UE011 in Table 4(a) was greater than 4 mm, the examination results conducted by the uncertified examiners were less than 1.0 (100%). Therefore, the regression analysis results in Fig. 6 showed the certified examiners had better capabilities than the uncertified examiners. However, the authors considered that the reliability of capability evaluation in a small difference of experimental data should be necessary. Thus, the authors attempted an additional evaluation in which the examination results at the defect height of UE008 and UE011 in Table 4(a) being virtually changed to 1.0 (100%). The original capabilities of the uncertified examiners were compared with a virtually changed capabilities of uncertified examiners on condition that POD of UE008 and UE011 are 1.0 (100%).

Eqs. (9) and (10) show the calculation results of the Model-1 and the Model-2 under the virtually changed data. Fig. 8(a) shows the regression analysis results of the Model-1 described by the Eqs. (3) and (9). Fig. 8(b) shows the regression analysis results of the Model-2 described by the Eqs. (4) and (10). The red circles are the experimental data of UE008 and UE011 conducted by the uncertified examiners. The green squares are the virtually changed data of UE008 and UE011. The yellow diamonds are the experimental data except UE008 and UE011 conducted by the uncertified examiners.

Model-1 on condition that POD of UE008 and UE011 are 1.0 (100%)

$$\begin{aligned} &POD(a) = 1 - \exp\left[-(a-\beta)\right] \\ &\beta_0 = 1.16, \quad \beta_{-95\%CL} = 0.683, \quad \beta_{+95\%CL} = 1.49 \\ &se_\beta = 0.173, \quad Se = 0.545 \end{aligned} \tag{9}$$

Model-2 on condition that POD of UE008 and UE011 are 1.0 (100%)

$$\begin{aligned} &POD(a) = \left[1 + \exp\left(-\beta 1 - \beta 2 \times a\right)\right]^{-1} \\ &\beta 1_0 = -19.0, \quad \beta 1_{-95\%CL} = \text{N/A}, \quad \beta 1_{+95\%CL} = -10.7 \\ &\beta 2_0 = 10.5, \quad \beta 2_{-95\%CL} = 6.04, \quad \beta 2_{+95\%CL} = \text{N/A} \\ &se_{\beta 1} = 5.66, \quad se_{\beta 2} = 3.08, \quad Se = 0.111 \end{aligned} \tag{10}$$

The comparison of the Model-1 equations between Eqs. (3) and (9) showed that it was not easy to decide the superiority of capabilities. The results of regression coefficients, 95% confidence intervals, standard error, and residual sum of squares were close in the equations. In contrast, the comparison of the Model-2 equations between Eqs. (4) and (10) showed that it was not difficult to decide the superiority of capabilities. Since the result of residual sum of squares in Eq. (4) was about twice as large as that in Eq. (10), Eq. (10) has higher capability than Eq. (4). In addition, the comparison of results of equation between Eqs. (4) and (10) as well as Fig. 8 (b) showed that the range of 95% confidence intervals in Eq. (10) was narrower than that in Eq. (4). Therefore, the additional evaluation showed the possibility of evaluation on UT examiners' capabilities under conditions of small difference on experimental data. Consequently, it was shown that the POD model with low residual sum of squares made it easier to evaluate the change of UT examiners' capabilities.

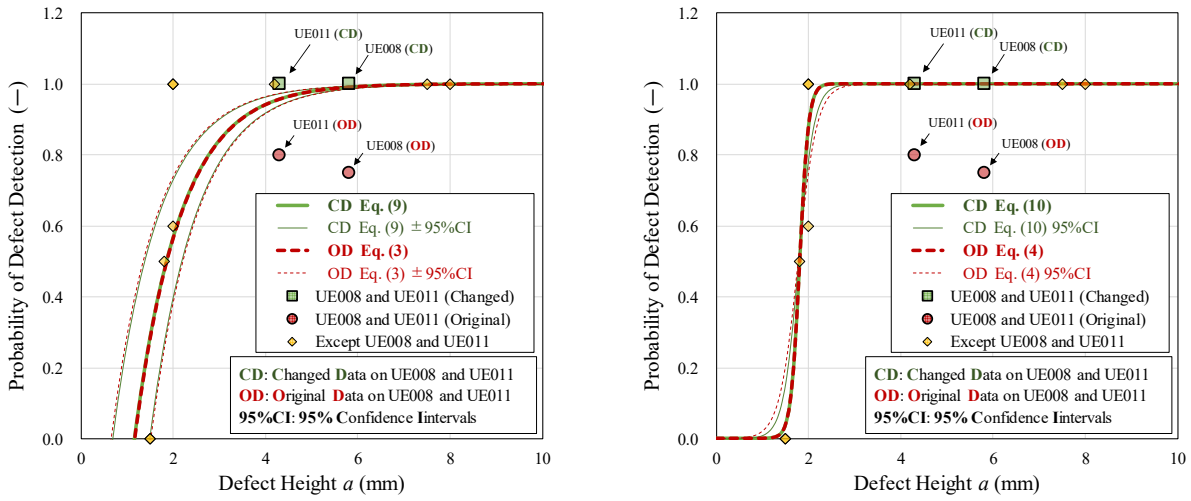

(a) Model-1 **(b) Model-2**

Fig. 8. POD results of (a) Model-1 and (b) Model-2 on the original vs. changed data of the uncertified examiners

4.2 Evaluation of failure risks of piping using cumulative failure probabilities

Fig. 7 showed the result that the cumulative failure probability increases as the inspection interval gets longer. The Model-2 had lower cumulative failure probabilities and narrower 95% confidence intervals than the Model-1 in inspection intervals of 4 and 6 years. However, Eqs. (7) and (8) showed the 95% confidence intervals for the Model-2 were only one side. Therefore, the authors

considered the 95% confidence intervals on both sides in the Model-2 should be necessary. The authors attempted additional regression analysis of Mode-2 on condition that $\beta 2$ is constant.

Here, Eq. (2) is transformed into Eq. (11). Fig. 9 shows a concept of Eq. (11) on condition that $\beta 2$ is constant. PODs of $\beta 1_0$, $\beta 1_{-95\%CL}$, and $\beta 1_{+95\%CL}$ are described as logistic curves (A), (B), and (C) in Fig. 9. The logistic curves (A), (B), and (C) pass through points P_0, $P_{-95\%CL}$, and $P_{+95\%CL}$. The points P_0, $P_{-95\%CL}$, and $P_{+95\%CL}$ are the inflection points of the logistic curves (A), (B), and (C). Additionally, the gradients of the tangent lines are parallel at the points P_0, $P_{-95\%CL}$, and $P_{+95\%CL}$.

Model-2

$$\begin{aligned} POD(a) &= \left[1+\exp\left(-\beta 1-\beta 2\times a\right)\right]^{-1} \\ &= \left(1+\exp\left\{-\beta 2\times\left[a-\left(-\beta 1/\beta 2\right)\right]\right\}\right)^{-1} \end{aligned} \tag{11}$$

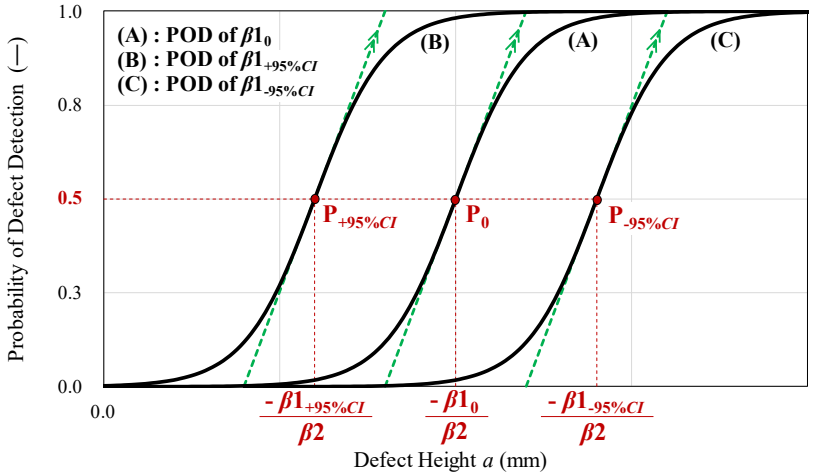

Fig. 9. Concept of Eq. (11) on condition that $\beta 2$ is constant

Eqs. (12) and (13) show the results of regression analysis of the Model-2 of the uncertified examiners and certified on condition that $\beta 2$ is constant. Fig. 10a shows the POD results. Fig. 10b shows the results of cumulative failure probability.

Model-2 of the uncertified examiners on condition that $\beta 2$ is constant

$$\begin{aligned} &POD(a) = \left(1+\exp\left\{-\beta 2\times\left[a-\left(-\beta 1/\beta 2\right)\right]\right\}\right)^{-1} \\ &\beta 1_0 = -19.0, \quad \beta 1_{-95\%CL} = -19.9, \quad \beta 1_{+95\%CL} = -17.8 \\ &\beta 2 = \beta 2_0 = 10.5\left(\text{constant}\right) \\ &Se_{95\%CL} = Se + F\times Ve = 0.213 + 4.96\times 0.0213 = 0.319 \\ &n = n_{UE} - n_1 = 11-1 = 10 \end{aligned} \tag{12}$$

Model-2 of the certified examiners on condition that $\beta 2$ is constant

$$\begin{aligned} &POD(a) = \left(1+\exp\left\{-\beta 2\times\left[a-\left(-\beta 1/\beta 2\right)\right]\right\}\right)^{-1} \\ &\beta 1_0 = -8.82, \quad \beta 1_{-95\%CL} = -10.3, \quad \beta 1_{+95\%CL} = -7.88 \\ &\beta 2 = \beta 2_0 = 8.93\left(\text{constant}\right) \\ &Se_{95\%CL} = Se + F\times Ve = 0.0252 + 4.84\times 0.00229 = 0.0362 \\ &n = n_{CE} - n_1 = 12-1 = 11 \end{aligned} \tag{13}$$

where, $Se_{95\%CL}$ is the residual sum of squares in Eqs. (12) and (13) in $\beta 1_{-95\%CL}$ and $\beta 1_{+95\%CL}$. Se is the residual sum of squares in Eq. (12) and Eq. (13) in $\beta 1_0$. Ve is the mean square for error in Eqs. (12) and (13) in $\beta 1_0$. F is the Snedecor's F-distribution in Eqs. (12) and (13) in $\beta 1_0$. n_1 is the number of the regression coefficient in Eqs. (12) and (13); since $\beta 2$ is as constant as $\beta 2_0$, $\beta 1$ is the only regression coefficient in Eqs. (12) and (13).

Figs. 7 and 10b showed that the POD model with low residual sum of squares had less uncertainty on the failure risks of piping. Hence, the superiority of the Model-2 in the cumulative failure probability result was shown as in the regression analysis result. Furthermore, Figs. 7 and 10b showed the results that the cumulative failure probabilities of both Model-1 and Model-2 performed by certified examiners in the inspection intervals of over 8 years were almost the identical values performed by uncertified examiners; therefore, it was shown that UT results performed by certified examiners might have equivalent failure risks of piping as UT results performed by uncertified examiners if an inspection interval gets longer.

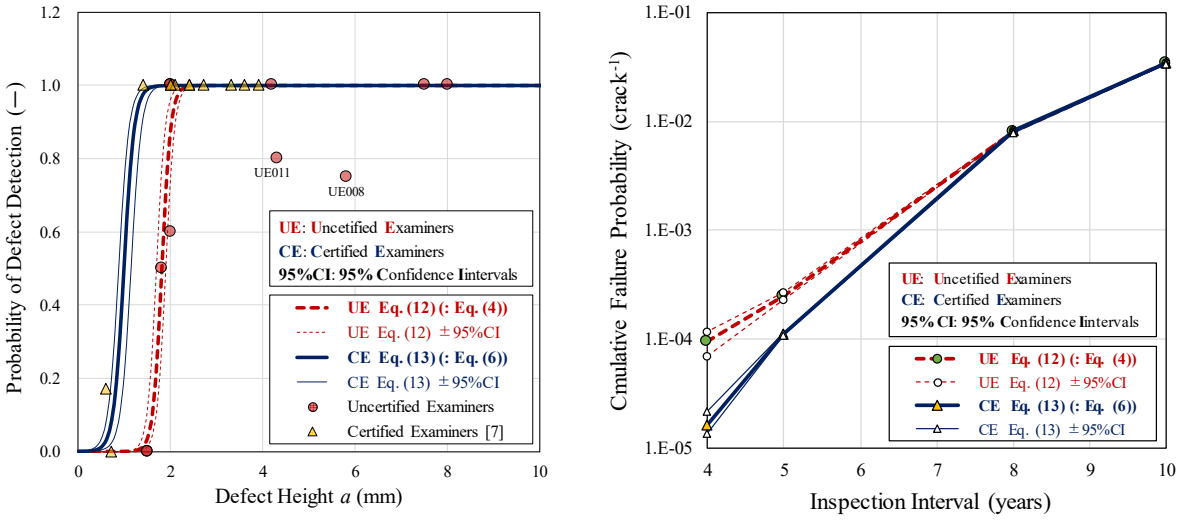

(a) PODs **(b) Cumulative failure probabilities**

Fig. 10. Results of (a) PODs and (b) cumulative failure probabilities on condition that $\beta 2$ is constant

5. Conclusions

The authors evaluated effects on the failure risks of piping using the cumulative failure probabilities and the POD models considering the difference of the UT examiners' capability. The conclusions from the evaluation are as follows:

(1) The POD model with low residual sum of squares made it easier to evaluate the change of the UT examiners' capabilities.
(2) The POD model with low residual sum of squares had less uncertainty on the failure risks of piping.
(3) UT results performed by certified examiners may have equivalent risks of piping as UT results performed by uncertified examiners if an inspection interval gets longer.

References

[1] The American Society of Mechanical Engineers: "ASME Boiler and Pressure Vessel Code – Rules for Inservice Inspection of Nuclear Power Plant Components –", ASME BPVC.XI-2015, pp. 78-124.
[2] H. Machida: "Influence of Non-Detective Examination Performance on Reliability of Pipes Having Stress Corrosion Cracks", Transactions of the Japan Society of Mechanical Engineers (JSME), Volume 77, Issue 782, pp. 1798-1813 (2011). (in Japanese)

[3] The Japan Society of Mechanical Engineers: “Code for Nuclear Power Generation Facilities – Rules on Fitness-for-Service for Nuclear Power Plants –”, JSME S NA1-2008. (in Japanese)
[4] H. Shohji, Y. Mizutani, T. Yoshida: "Study of Crack Detection Probability for Maintenance Reliability of Power Plant (Estimation of Crack Detection Probability on the Damage Probability)", The Japan Society of Mechanical Engineers (JSME), Volume 83, Issue 845 (2017). (in Japanese)
[5] P. G. Heasler, S. R. Doctor: "Piping Inspection Round Robin; 5.0 Relationship Between Detection and Crack Size", U. S. Nuclear Regulatory Commission, NUREG/CR-5068, PNNL-10475, pp. 5.1-5.29 (1996).
[6] H. Machida: "Reliability Assessment of PLR Piping Based on Domestic SCC Data", The ASME 2007 Pressure Vessels and Piping Division Conference, San Antonio, Texas, USA, July 22-26, PVP2007-26059 (2007).
[7] Japan Nuclear Energy Safety Organization (JNES): "Report on Demonstration Project of Inspection Technique at Nuclear Power Facility (Confirmation of Accuracy for Defect Detection and Sizing on Ultrasonic Testing) [Summary Version]" [Translated from Japanese.], 05KIZAIHOU-0001, pp. 658-714 (2005). (in Japanese)
[8] The Japan Electric Association: "The Ultrasonic Examination Guideline for In-Service Inspection of Light Water Cooled Nuclear Power Plant Components" [Translated from Japanese.], JEAC 4207-2008. (in Japanese)
[9] JIS Z 2345-1: "Standard Test Blocks for Ultrasonic Testing - Part 1: A1 Standard Test Block".
[10] The Japan Electric Association: "The Ultrasonic Examination Guideline for In-Service Inspection of Light Water Cooled Nuclear Power Plant Components" [Translated from Japanese.], JEAC 4207-2004.
[11] H. W. Bargmann: "Pressure Vessel Integrity in the Presence of Defects: The Probabilistic Prediction in Spite of Scarce Data", Nuclear Engineering Design 93, pp. 289-294 (1986).
[12] T. Haga: "Statistical Analysis for Pharmaceutical Drug Development - Part 3: Nonlinear Model Revised Edition" [Translated from Japanese.], Scientist Press Company Limited, pp. 1-24 (2016). (in Japanese)
[13] Y. Sakiyama, K. Ohashi, Y. Takahashi: "Application of Nonlinear Regression Model to Sigmoid Dose-Response Relationship in Pharmacological Studies", Folia Pharmacologica Japonica, Volume 132, Issue 4, pp. 199-206 (2008). (in Japanese)
[14] S. Yoshimura, Y. Kanto: "Probabilistic Fracture Mechanics for Risk-Informed Activities – Fundamentals and Applications –", Probabilistic Fracture Mechanics Subcommittee, Atomic Energy Research Committee, The Japan Welding Engineering Society, pp. 1-94 (2017).
[15] H. Itoh, D. Kato, K. Osakabe, H. Nishikawa, K. Onizawa: "User’s Manuals of Probabilistic Fracture Mechanics Analysis Code for Aged Piping, PASCAL-SP", Reactor Safety Research Unit, Nuclear Safety Research Center, Japan Atomic Energy Agency, pp. 1-48 (2010). (in Japanese)
[16] M. Arakawa, K. Narumi, H. Machida, K. Onizawa: "Benchmark Analysis on the Failure Probability Assessment of Piping with Stress Corrosion Cracks", The ASME 2011 Pressure Vessels and Piping Division Conference, Baltimore, Maryland, USA, July 17-21, PVP2011-57498 (2011).
[17] H. Machida, N. Yamashita: "Effect of Crack Detection Performance and Sizing Accuracy on Reliability of Piping with Stress Corrosion Cracks", The ASME 2008 Pressure Vessels and Piping Division Conference, Chicago, Illinois, USA, July 27-31, PVP2008-61017 (2008).
[18] Ministry of Economy, Trade and Industry: "Integrity Evaluation Method for Reactor Recirculation Piping (Draft)" [Translated from Japanese.], 10th Conference of Task-Force on Structural Integrity of Nuclear Power Generation Facility, Sub-Committee on Nuclear Safety and Security, Research Committee on Natural Resource and Energy, Agency for Natural Resource and Energy, METI, June 15th, Reference Paper 10-7, pp. 12-21 (2004). (in Japanese)
[19] Ministry of Economy, Trade and Industry: "Evaluation Example of Integrity of Primary Loop Recirculation System Piping Based on the Evaluation Result of the Improved Ultrasonic Testing Accuracy" [Translated from Japanese.], 9th Conference of Task-Force on Structural Integrity of Nuclear Power Generation Facility, Sub-committee on Nuclear Safety and Security, Research Committee on Natural Resource and Energy, Agency for Natural Resource and Energy, METI, September 1st, Conference Material 9-6 (2003). (in Japanese)
[20] M. Nagai, N. Miura, H. Shohji: "Piping Integrity Assessment Utilizing Probability Fracture Mechanics - Effect of Probability of Detection Failure Probability -", Central Research Institute of Electric Power Industry (CRIEPI), CRIEPI Research Report Q16007 (2017). (in Japanese)